Dual-Output Buck Converters with Multivariable Control of Single-Inductor

Venkatraman.E1, Raja.P2,

PG scholar1, Asst Professor 2, Department of EEE, Arunai College of Engineering, Thiruvannamalai.

Abstract: *Cross regulation is the main technical drawback of a Single-Inductor Multiple-Output (SIMO) dc-dc converter. This paper proposes a multivariable digital controller to suppress the cross regulation of a Single-Inductor Dual-Output (SIDO) buck converter in Continuous Conduction Mode (CCM) operation. The controller design methodology originates from the open-loop shaping of the Multi-Input Multi-Output (MIMO) systems. The control design procedure includes: (i) determination of the non-parametric model of a SIDO buck converter at its rated operating point, (ii) determination of the class of the controller, and (iii) converter open-loop shaping by convex minimization of the square second norm of the error between the converter open-loop transfer function and a desired open-loop transfer function. The proposed controller minimizes the coupling between the outputs of the SIDO buck converter and provides satisfactory dynamic performance in CCM operation. This paper describes the theoretical aspects involved in the design procedure of the controller and evaluates the performance of the controller based on simulation studies and experiments.*

I. Introduction

SINGLE-Inductor Multiple-Output (SIMO) dc-dc convert-ers have attracted increasing interest for the applications where multiple independent supply voltage levels are required. As compared with multiple independent dc-dc converters, a SIMO converter only uses one single inductor to generate multiple voltage levels. Therefore, in terms of the cost, footprint, and conversion efficiency, a SIMO converter provides a superior solution. In spite of its merits, a SIMO converter suffers from functional interdependency among its parameters such as output voltages, dc voltage gains, and load currents. Con-sequent, proper operation of a SIMO converter necessitates a sophisticated cross regulation suppression strategy to de-couple the output voltage levels [1]–[9]. This paper aims at development of a cross regulation suppression strategy for a Single-Input Dual-Output (SIDO) buck converter in Continuous Conduction Mode (CCM) operation.

Cross regulation of a SIMO converter has been investigated and reported in the technical literature, and correspondingly, various remedial measures have been proposed/implemented to resolve it. The proposed/investigated methods are mainly based on the following approaches:

- The first approach is based on using a time multiplexing control technique in Discontinuous Conduction Mode (DCM) [9], [10]. Although this approach suppresses cross regulation, the large amplitude of the inductor current ripples under heavy load conditions impacts the performance of the converter, e.g., voltage ripples, switching noise, and dynamic response.
- The second approach is based on using a free wheel switching control technique in Pseudo-Continuous Con-diction Mode (PCCM) [7], [11]. In this approach, an additional switch is added to the converter circuit which enables the converter to handle large currents of heavy loads as well as cross regulation suppression. The main drawback of this approach is that due to the additional switch, the converter switching loss and footprint are increased.
- The third approach is based on using a decoupled control technique in Continuous Conduction Mode (CCM) [4], [12], [13]. As compared with the previous approaches, this approach requires a more elaborate control strategy/algorithm. However, in terms of power stage design and efficiency, this approach provides a viable approach to address the main technical issue of a SIMO converter.

This paper proposes a general digital multivariable controller design methodology for the voltage control of a SIDO buck converter in CCM. The proposed method originates from the open-loop shaping of the Multi-Input Multi-Output (MIMO) systems presented in [14] which uses MIMO non-parametric or spectral model of the converter for the rated operating point along with a linearly parameterized MIMO controller to form the open-loop transfer function matrix.

Based on the dynamic performance and decoupling requirements, a desired open-loop transfer function matrix is formed, and its diagonal and off-diagonal elements are determined. Minimizing the error between the open-loop transfer function matrix and the
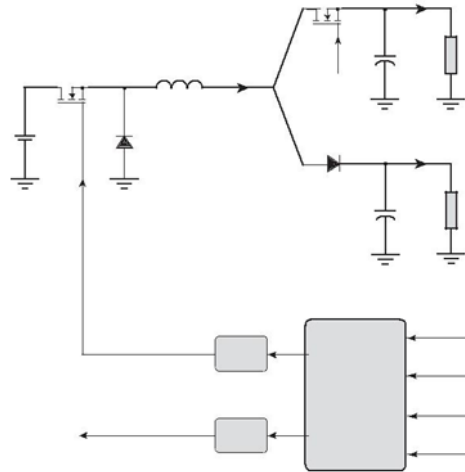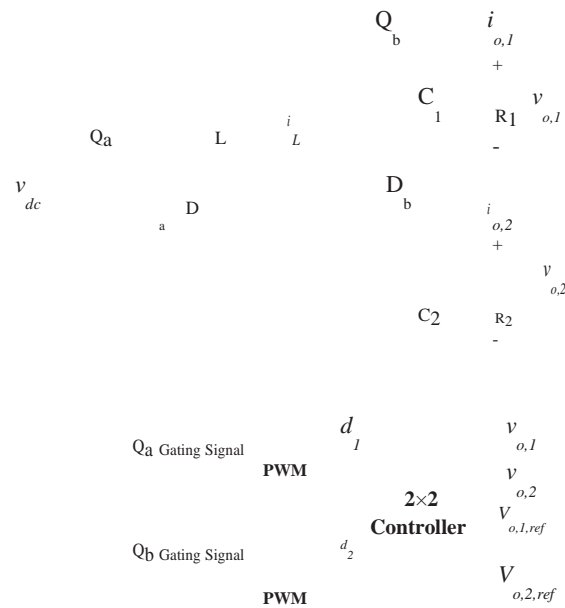
Fig. 1. Circuit diagram of a SIDO buck converter.

where $0 < d_1 < 1$ and $0 < d_2 < 1$. Solving equations (1a) and (1b), the duty cycles d_1 and d_2 are determined by

$$d_1 = \frac{I_{o,1}}{I_{o,1} + I_{o,2}}, I_{o,1} + I_{o,2} = I_L, \qquad (2a)$$

$$d_2 = \frac{V_{o,1}[d_2^2 R_1 + (1 - d_2)^2 R_2]}{V_{in} d_2 R_1}. \qquad (2b)$$

B. Cross Regulation

The open-loop control-to-output transfer functions of the SIDO buck converter of Fig. 1 are expressed by [13]:

$$\begin{bmatrix} v_{o,1}(s) \\ v_{o,2}(s) \end{bmatrix} = \begin{bmatrix} G_{d11}(s) & G_{d12}(s) \\ G_{d21}(s) & G_{d22}(s) \end{bmatrix} \begin{bmatrix} d_1(s) \\ d_2(s) \end{bmatrix}, \qquad (3)$$

where

$$G_{d11}(s) = \frac{v_{o,1}(s)}{d_1(s)} = \frac{V_{in} d_2 Z_{eq1}(s)}{\delta(s)},$$

$$\frac{v_{o,2}(s)}{} \qquad V_{in}(1 - d_2) Z_{eq2}(s)$$

$$G_{d21}(s) = \frac{ = }{d_1(s) \delta(s)}, G_{d12}(s) =$$

$$= \frac{I_L R_{eq1}(s)[(1-d_2)Z_{eq2}(s)+sL]+d_2 Z_{eq1}(s)(V_{o,2}-V_{o,1})}{\delta(sv_{o,2}(s)}$$

Then the desired dynamic performance, while simultaneously, the off-diagonal elements are designed to decouple the output voltages. To ensure the stability of the designed controller, the minimization problem is subject to a few mathematical constraints. Performance of the proposed controller is studied based on time-domain simulation and is experimentally vali-dated.

The rest of this paper is organized as follows. Section II describes the basics of the operation of a SIDO buck converter. Section III presents the design procedure of the proposed multivariable controller. Section IV proposes a multivariable voltage controller for a SIDO buck converter. The performance evaluation of the proposed controller, under various operating scenarios, is reported in Section V. Section VI concludes the paper.

II. Sido Buck Converter

A. Basics of Operation

Fig. 1 shows a circuit diagram of a SIDO buck converter with two output voltages, $v_{o,1}$ and $v_{o,2}$, where $v_{o,1} > v_{o,2}$. The output voltages $v_{o,1}$ and $v_{o,2}$ are regulated by adjusting the duty cycles d_1 and d_2. The duty cycle of the input switch S_1, i.e., d_1, regulates the total input power of the SIDO buck converter, and consequently, the inductor current i_L. The duty cycle of the output switch S_2, i.e., d_2, determines how the inductor current i_L is divided between the two outputs [13]. Assuming ideal switches and diodes, the mathematical equations which govern steady-state behavior of the converter, are

$$\frac{V_{o,1}}{V_{in}} = \frac{d_1 d_2 R_1}{d^2 R_1 + (1-d_2)^2 R_2}, \qquad (1a)$$

$$\frac{V_{o,2}}{V_{in}} = \frac{d_1(1-d_2)R_2}{d^2 R_1 + (1-d_2)^2 R_2}, \qquad (1b)$$

$$= -\frac{I_L R_{eq2}(s)[d_2 Z_{eq1}(s)+sL]+(1-d_2)Z_{eq2}(s)(V_{o,1}-V_{o,2})}{\delta(s)}$$

$$Z_{eq1}(s) = R_1 - \frac{1}{sC_1}, Z_{eq2}(s) = R_2 - \frac{1}{sC_2}$$

and

$$\delta(s) = d_2{}^2 R_{eq1} + d_2{}^{-2} R_{eq2} + sL.$$

Equation above represents the transfer function matrix of a typical 2x2 MIMO system in which due to the non-zero off-diagonal terms in the transfer matrix, there exist a coupling between the output and input control loops. In the following section, a multivariable design methodology for the voltage control of the SIDO buck converter of Fig. 1 is proposed.

III. The Multivariable Controller Design Methodology

This section proposes a methodology to design a voltage controller for a SIDO buck converter. The proposed method-ology originates from the MIMO controller design approach in [14], which based on the spectral MIMO model of a system, develops a convex optimization-based control method. The basic idea of the proposed approach is to shape the open-loop transfer function matrix of a MIMO system by minimizing the absolute error between the open-loop trans-fer function matrix of the system, obtained at an operating point of interest, i.e., $\mathbf{L}(j\omega)$; $\omega \in R$, and a desired open-loop transfer function matrix, i.e., $\mathbf{L_d}(s)$. The overall system open-loop transfer function matrix at the operating point of interest is $\mathbf{L}(j\omega) = \mathbf{G}(j\omega)\mathbf{K}(j\omega)$, where $\mathbf{G}(j\omega)$ represents the system transfer function matrix at the operating point of interest, and $\mathbf{K}(j\omega)$ represents the controller transfer function matrix. Since this loop shaping approach does not necessarily guarantee the desired performance and stability of the closed-loop system, to ensure the stability and to meet performance specifications, the minimization problem is subject to a few mathematical constraints. In the next subsection, the detailed design procedure of the controller is described. The procedure includes the following main steps: (i) determination of the non-parametric model of the system at the rated operating point, (ii) determination of the class of the controller, and (iii) system open-loop shaping by the minimization of the summation of the square

second norm of the error between the system open-loop transfer function matrix and a desired open-loop transfer function matrix.

A. Determination of the Non-parametric Model

Assuming a system with two inputs and two outputs, the transfer function matrix of the system at an arbitrary operating Point, based on non-parametric models, is given by: The elements of the matrix $\mathbf{G}(j\omega)$ are determined by frequency response measurements of the system, i.e., the estimation of the frequency response of the system in the range of the frequencies of interest. To achieve this, one can adopt the system transfer function matrix of (3) and derive the frequency response of the system for any operating point of interest.

B. Determination of the Class of controller

To form the open-loop transfer function matrix of the overall system including the controller, the class of the to-be-designed controller is required. Since the objective is to design a linearly parameterized multivariable digital controller, the class of the controller is determined in the z-domain. A generic form of such a multivariable discrete-time controller in the z-domain is given by:

$$\mathbf{G}(j\omega) = \overline{\quad G_{21}(j\omega) \quad G_{22}(j\omega)\_},$$

C. Loop Shaping by Convex Optimization

The loop shaping of the open-loop transfer function matrix of the system is carried out by minimizing the square second norm of the error between the matrix $\mathbf{L}$ and a desired open-loop transfer function matrix, $\mathbf{L_D}(s)$. Consequently, the control design procedure is turned to an optimization problem as follows [14]:

$$\min \_ \mathbf{L}(\rho) - \mathbf{L_D} \_^2, \qquad (11)$$

$$\mathbf{D}(s) = \begin{bmatrix} L_{D1}(s) & 0 \\ 0 & L_{D2}(s) \end{bmatrix} = \begin{bmatrix} \dfrac{\omega_c}{s} & 0 \\ 0 & \dfrac{\omega_c}{s} \end{bmatrix}. \qquad (12)$$

In the transfer function matrix of (12), the off-diagonal elements are set at zero to decouple the system while the diagonal elements are tuned to provide a satisfactory dynamic response by adjusting ω_c. Furthermore, the closed-loop sensitivity func-tion of the diagonal elements, $S = (1 + L_{qq})^{-1}$, can be shaped using $W_1(j\omega)S(j\omega) < 1 \; \forall \omega \in \mathbb{R}$, where $W_1(j\omega)$ is a weighting filter. This is an H_∞ performance condition that guarantees the robustness of the main axes [14]. A convex approximation of this condition can be given by the following linear constraints [14]:

$$|W_1(j\omega)[1 + L_{Dq}(j\omega,\rho)]| -$$
$$Re \{[1 + L_{Dq}(-j\omega)][1 + L_{qq}(j\omega,\rho)]\} < 0$$
$$\forall \omega \in \mathbb{R}, \text{ and } q = 1,2. \qquad (13)$$

$$\mathbf{K}(j\omega) = \begin{bmatrix} K_{11}(j\omega) & K_{12}(j\omega) \\ K_{21}(j\omega) & K_{22}(j\omega) \end{bmatrix}. \qquad (6)$$

Each element of the controller matrix of (6) is then given by:

$$K_{ij}(j\omega,\rho) = \rho_{ij}^T\varphi(j\omega), \qquad (7)$$

where

$$\rho_{ij}^T = [\rho_0,\rho_1,\rho_2,...,\rho_n], \qquad (8)$$

and $\varphi(j\omega)$ is the frequency response of

$$\varphi^T(z) = \left[\frac{1}{1-z^{-1}}, \frac{z^{-1}}{1-z^{-1}}, \frac{z^{-2}}{1-z^{-2}},..., \frac{z^{-n}}{1-z^{-1}} \right], \qquad (9)$$

Computed by replacing $z = e^{-j\omega}$. n in (8) and (9) represents the number of the controller parameters for each element of the controller matrix.

Given the non-parametric model of the system by (5) and the defined controller class by (6), the open-

loop transfer function matrix of the overall system is given by:

$$\mathbf{L}(j\omega) = \mathbf{G}(j\omega)\mathbf{K}(j\omega); \omega \in \{R\}. \quad (10)$$

Solving the optimization problem of (11) constrained to (13) results in a decoupled open-loop transfer function ma-trix, which provides satisfactory reference tracking capability. However, it does not guarantee the stability of the multivari-able closed-loop system. To ensure the stability of the system, the Generalized Nyquist Stability criterion must be respected. This criterion guarantees the stability of the feedback system *if and only if the net sum of counterclockwise encirclements of the critical point $(-1 + j0)$ by the set of eigenvalues of the matrix $\mathbf{L}_i(j\omega)$ is equal to the total number of the right-half plane poles of $\mathbf{L}_i(s)$.* To satisfy this condition, adopting *Gershgorin bands*, the reference [14] proves that assuming the non-parametric model $\mathbf{G}_i(j\omega)$, the linearly parameterized controller $\mathbf{K}(z)$ defined in (7) stabilizes the closed-loop system

$$r_q(\omega, \rho) - \frac{Re\left\{[1 + L_{Dq}(-j\omega)][1 + L_{qq}(j\omega, \rho)]\right\}}{|1 + L_{Dq}(j\omega)|} < 0$$

$$\forall \omega \in R \; for \, q = 1,2. \quad (14)$$

where, $r_1(\omega, \rho)$ and $r_2(\omega, \rho)$ are defined as:

$$r_1(\omega, \rho) = |L_{21}(j\omega, \rho)| \quad (15)$$

$$, \rho) = |L_{12}(j\omega, \rho)|. \quad (16)$$

In (14), the diagonal matrix $\mathbf{L}_D(j\omega)$ In (14), the diagonal matrix $\mathbf{L}_D(j\omega)$ should be chosen such that The optimization problem of (21) in conjunction with the should be chosen such that number of counterclockwise encirclements of the critical point by the Nyquist plot of the set of its eigenvalues is equal to the number of unstable poles of $\mathbf{G}(\mathbf{s})$. For example, the transfer function matrix of (12) is a fulfilling choice. Considering the constraints for the desired performance given by (13) and the constraints for the stability of the closed-loop system given by (14), the design procedure is summarized into the following optimization problem:

$$\min \_ \mathbf{L}(\rho) - \mathbf{L_D} \_^2,$$

where $\_ . \__F$ is the Frobenius norm. Therefore, the following optimization problem is deduced. constraints in (22) and (23) is used as a basis to determine the coefficients of the MIMO controller, which is the subject of the next section.

$$\min \_ \mathbf{L}(j\omega_k, \rho) - \mathbf{L_D}(j\omega_k) \__F, \quad (21)$$

subject to

$$|W_1(j\omega_k)[1 + L_{Dq}(j\omega_k)]| -$$
$$Re\,[1 + L_{Dq}(-j\omega_k)][1 + L_{qq}(j\omega_k, \rho)] < 0$$
$$for \, k = 1,...,N, \, and \, q = 1,2. \quad (22)$$

and

$$r_q(\omega_k, \rho) - \frac{Re\left\{[1 + L_{Dq}(-j\omega_k)][1 + L_{qq}(j\omega_k, \rho)]\right\}}{|1 + L_{Dq}(j\omega_k)|} < 0$$
$$for \, k = 1,...,N, and \, q = 1,2. \quad (23)$$

here $\omega_c = 2.5e5 \frac{rad}{s}$. The zero off-diagonal elements of $\mathbf{L}_D$ are to eliminate the cross coupling between the output volt-ages. Solving the minimization problem of (21), the controller transfer function matrix is calculated as:

$$\mathbf{K}(z) = K_{11}(z) \quad K_{12}(z) , \tag{26}$$

$$K2_1(z) \quad K_{22}(z)$$

Where

$$K_{11}(z) = \frac{1.29 \quad -+ \quad - \quad + \quad 0.33z^{-4} \quad -}{3.31z^{-1} \quad 3.07z^{-2} \quad 1.32z^{-3} \quad 0.03z^{-5}} \Big/ (1 - z^{-1}),$$

$$K_{12}(z) = \frac{1.41 \quad -+ \quad - \quad + \quad 0.34z^{-4} \quad -}{3.41z^{-1} \quad 3.07z^{-2} \quad 1.34z^{-3} \quad 0.03z^{-5}} \Big/ (1 - z^{-1}),$$

$$K_{21}(z) = \frac{0.71 \quad -- \quad - \quad}{0.56z^{-1} \quad 0.08z^{-2} \quad 0.01z^{-3} + 0.02z^{-4} - 0.005z^{-5}} \Big/ (1 - z^{-1}),$$

$$K_{22}(z) = \frac{-0.60 + 0.54z^{-1} - 0.02z^{-2} + 0.07z^{-3} - 0.04z^{-4} + 0.007z^{-5}}{1 - z^{-1}}.$$

IV. The Proposed Multivariable Voltage Controller

In this section, the multivariable controller design method ology of Section III is used to design a multivariable voltage controller for the SIDO buck converter of Fig. 1. Based on the design procedure described in Section III, the first step is to obtain the non-parametric model of the system at an operating point for which the controller is designed. In this paper, the spectral model of the system corresponding to the rated currents of the two outputs is derived and used in the design procedure. The second step is to determine the class of the controller.

The primary goal of the controller is to stabilize the system and to regulate the voltages within a large robustness margin, with a fast dynamic response and zero steady-state error. Therefore, each element of the controller matrix must containsan integrator.

, in order to achieve a large robustness margin, one can increase the order of the controller. Therefore, the individual elements of the transfer function matrix of the two-input two-output controller can be selected as in which n can be any integer number and is determined based on the required dynamic response and/or robustness w.r.t. to load parameters variations.

In this paper, n is chosen to be 5. The coefficients of the individual elements of the controller transfer function matrix, i.e., ρ_0, ρ_1, ρ_2, ..., and ρ_n are determined in the third step of the control design methodology, i.e., solving the constrained minimization problem. To solve the constrained minimization problem of (21), a desired open- loop transfer function matrix is required. A reasonable open- loop transfer function matrix for this application is considered.
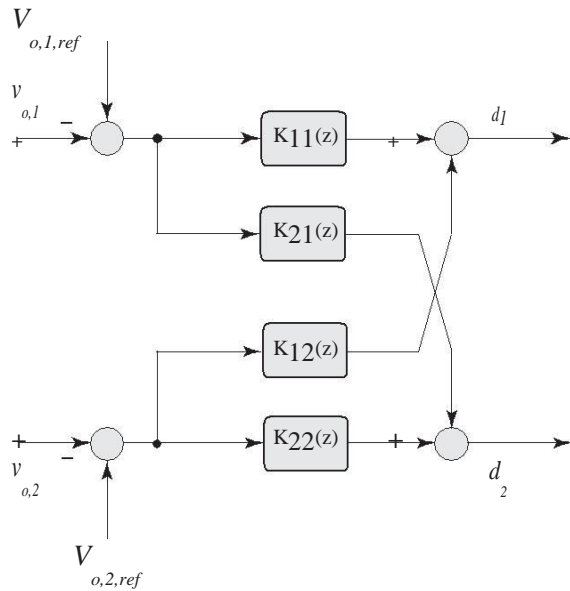
The block diagram of the controller is shown in Fig. 2.
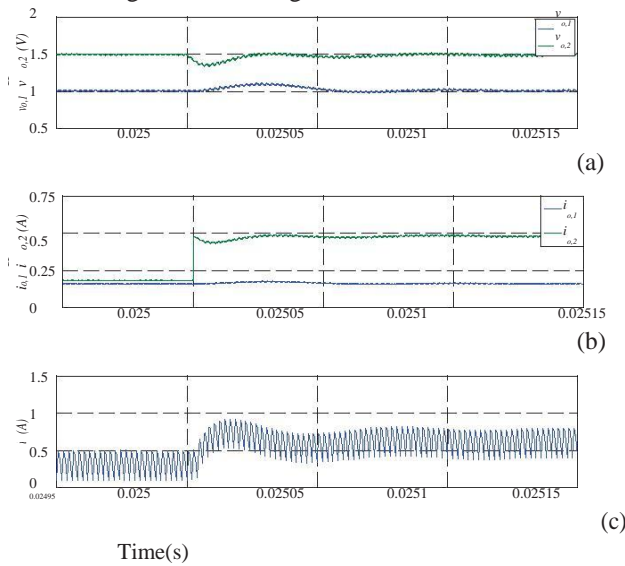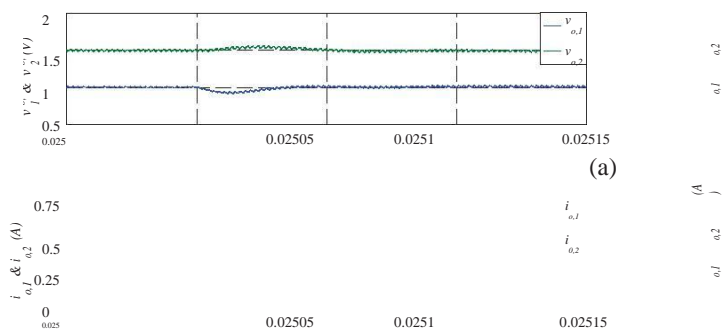

Fig. 2. Block diagram of the controller.

(a)

(b)

(c)

Time(s)

Fig.3. Simulation response of the SIDO buck converter to a step change in $i_{o,2}$ from 180 mA to 470 mA and $i_{o,1}$=160 mA: (a) output voltages, (b) load currents, and (c) inductor current.
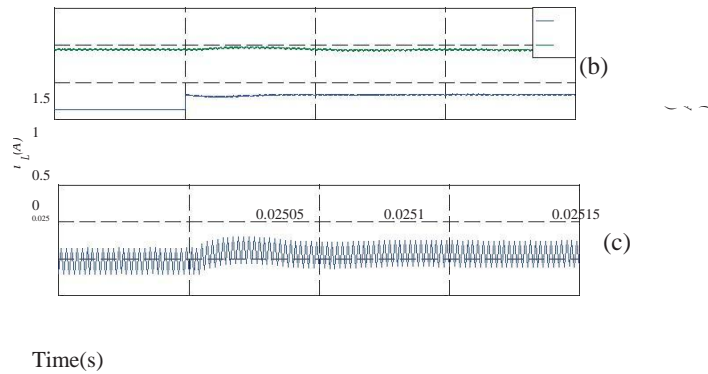

(a)

Time(s)

Fig. 4. Simulation response of the SIDO buck converter to a step change in $I_{o,1}$ from 100 mA to 160 mA and $I_{o,2}$=470 mA: (a) output voltages, (b) load currents, and (c) inductor current.
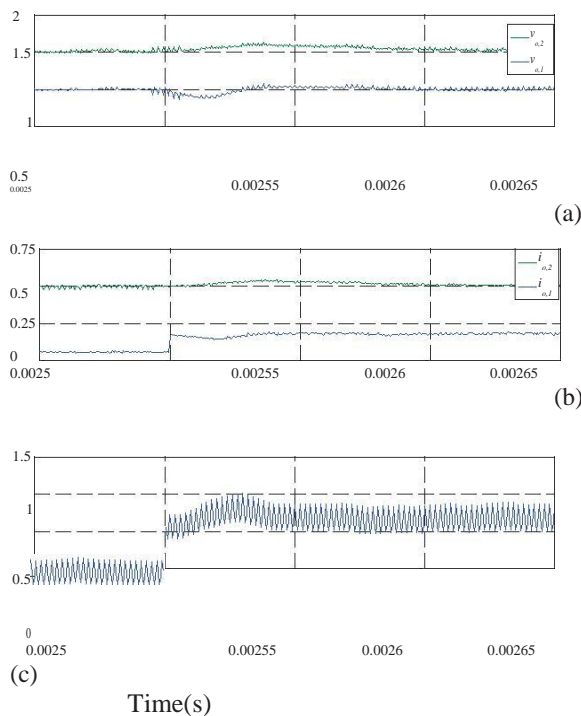

Time(s)

Fig. 5. Experimental response of the SIDO buck converter to a step change in $i_{o,1}$ from 100 mA to 160 mA and $i_{o,2}$=470 mA: (a) output voltages, (b) load currents, and (c) inductor current.

V. Performance Evaluation

A. Simulation Results

The SIDO buck converter of Fig. 1 that operates based on the proposed control strategy is simulated in the MAT-LAB/SIMULINK environment. The converter parameters are $V_{dc} = 5V$, $L = 5\mu H$, $C_1 = 10\mu F$, $C_1 = 10\mu F$, $f_s = 500kHz$, $V_{o,1} = 1V$, $V_{o,2} = 1.5V$, and $I_{o,1} = I_{o,2} = 0 : 500mA$. The sampling frequency is equal to the switching frequency. Two case studies are conducted as follows:

Case 1: Initially the SIDO buck converter is in a steady state mode of operation and $i_{o,1} = 100$ mA and $i_{o,2} = 470$ mA. At $t = 0.025s$, $i_{o,1}$ is stepped up from 100 mA to 160 mA while the current of the second output is kept constant. Figs. 3 (a), (b), and (c) show the output voltages, currents, and the inductor current, respectively. As Fig. 3 shows, subsequent to the step change in the load current $i_{o,1}$, the output voltage $v_{o,2}$ goes under a negligible transient which quickly settles down. The results of Fig. 3 highlights the capability of the proposed controller in effectively suppressing the coupling between the output voltages of the converter with a satisfactory dynamic response

Case 2: Initially the SIDO buck converter is in a steady state mode of operation and $i_{o,1} = 160$ mA and $i_{o,2} = 180$ mA. At $t = 0.025s$, $i_{o,2}$ is stepped up from 180 mA to 470 mA while the current of the first output is kept

constant. The results are reported in Fig. 4. As shown in Fig. 4, subsequent to the load current transient at the second output, voltage regulation at the the two outputs are ensured and the first output voltage reach its steady-state value with a short settling time.

B. Experimental Results

To experimentally evaluate the performance of the proposed control strategy, a SIDO buck converter prototype is imple-mented. The circuit parameters are the same as those used in simulation studies. The control strategy is implemented in a fully digital control platform based on the National Instruments Compact RIO system.

The experimental transient responses of the SIDO buck converter to the load current step-up changes corresponding to Case 1 and Case 2 of the simulation results are shown in Figs. 5 and 6, respectively. The experimental results of Figs. 5 and 6 are closely matched with their corresponding simulation results in Figs. 3 and 4. The results of Figs. 3 to 6 confirm the effectiveness of the proposed multivariable controller to effectively decouple the output voltages of a SIDO buck converter at various operating points in CCM operation.

VI. Conclusion

This paper proposes a multivariable controller design methodology for the voltage control of a SIDO buck converter in CCM operation. The proposed methodology is based on shaping the open-loop MIMO transfer function matrix of the converter by (i) obtaining a non-parametric model of the converter at an operating point of interest, e.g., at the rated load conditions, (ii) determination of the class of the controller, and (iii) determination of the coefficient of the controller by solving a convex optimization problem. The simulation and experimental results confirm satisfactory performance of the proposed multivariable controller in cross regulation suppression of the output voltages of a SIDO buck converter.

Reference

[1]. H.-P. Le, C.-S. Chae, K.-C. Lee, S.-W. Wang, G.-H. Cho, and G.-H. Cho, "A single-inductor switching dc-dc converter with five outputs and ordered power-distributive control," *IEEE Journal of Solid-State Circuits*, vol. 42, no. 12, pp. 2706–2714, December 2007.

[2]. D. Kwon and G. A. Rincon-Mora, "Single-inductor- multiple-output switching dc-dc converters," *IEEE Transactions on Circuits and Systems-*

[3]. M.-H. Huang and K.-H. Chen, "Single-inductor multi-output (SIMO) dc-dc converters with high light-load efficiency and minimized cross-regulation for portable devices," *IEEE Journal of Solid-State Circuits*, vol. 44, no. 4, pp. 1099–1111, April 2009. Z. Shen, X. Chang, W. Wang, X. Tan, N. Yan, and [4] H. Min, "Predictive digital current control of single-inductor multiple-output converters in CCM with low cross regulation," *IEEE Trans. on Power Electronics*, vol. 27, no. 4, pp. 1917–1925, April 2012.

[4]. M.-H. Huang, Y.-N. Tsai, and K.-H. Chen, "Sub-1 v input single-inductor dual output (SIDO) dc-dc converter with adaptive load tracking control (ALTC) for single-cell powered systems," *IEEE Transactions on Power Electronics*, vol. 25, no. 7, pp. 1713–1724, July 2010.

[5]. P. Patra, A. Patra, and N. Misra, "A single-inductor multiple-output switcher with simultaneous buck, boost and inverted outputs," *IEEE Transactions on Power Electronics*, vol. 27, no. 4, pp. 1936–1951, April.2012.

[6]. S.-C. Koon, Y.-H. Lam, and W.-H. Ki, "Integrated charge -control single-inductor dual-output step-up / step-down converter," *IEEE International Symposium on Circuits and Systems*, pp. 3071–3074, 2005.

[7]. B. Tsai, O. Trescases, and B. Francis, "An investigation of steady-state averaging for the single-inductor dual-output buck converter using fourier analysis," *Control and Model for Power Electronics*, pp. 1–5, June 2010.

[8]. H. Chen, Y. Zhang, and D. Ma, "A SIMO parallel-string driver IC for dimmable led backlighting with local bus voltage optimization and single time-shared regulation loop," *IEEE Transactions on Power Electronics*, vol. 27, no. 1, pp. 452–462, January 2012.

[9]. D. Ma, W.-H. Ki, C.-Y. Tusi, and P. Mok, "Single-inductor multiple out-put switching converters with time-multiplexing control in discontinous mode," *IEEE J. Solid-State Circuits*, vol. 38, no. 1, pp. 89–100, Jan. 2003.

[10]. D. Ma, W.-H. Ki, and C.-Y. Tusi, "A pesudo-CCM/DCM SIMO switch-ing converter with freewheel switching," *IEEE J. Solid-State Circuits*, vol. 38, no. 6, pp. 1007–1014, Jun. 2003.

[11]. D. Tervisan, P. Mattavelli, and P. Tenti, "Digital control of single-inductor multiple-output step-down dc-dc converters in CCM," *IEEE Transactions on Industrial Electronics*, vol. 55, no. 9, pp. 3476–3483, September 2008.

[12]. K.-Y. Lin, C.-S. Huang, D. Chen, and K. H. Liu, "Modeling and design of feedback loops for a voltage-mode single-inductor dual output buck converter," *Power Electronics Specialists Conference*, pp. 3389–

3395, June 2008.

[13]. G. Galdos, A. Karimi, and R. Longchamp, "H_∞ controller design for spectral MIMO models by convex optimization," *Journal of Process Control*, vol. 20, no. 10, pp. 1175–1182, 2010.

[14]. J. Sturm, "Using sedumi 1.02, a matlab toolbox for optimization over symmetric cones," *Optimization Methods and software*, vol. 11, pp. 625– 653, 1999.